

# Origin and evolution of circular waves and spirals in *Dictyostelium discoideum* territories

(cellular slime molds/phosphodiesterase/morphogenesis/phosphodiesterase inhibitor/self organization)

EIRÍKUR PÁLSSON\*† AND EDWARD C. COX†

\*Program in Applied and Computational Mathematics, †Department of Molecular Biology, Princeton University, Princeton, NJ 08544

Communicated by J. T. Bonner, Princeton University, Princeton, NJ, November 3, 1995

**ABSTRACT** Randomly distributed *Dictyostelium discoideum* cells form cooperative territories by signaling to each other with cAMP. Cells initiate the process by sending out pulsatile signals, which propagate as waves. With time, circular and spiral patterns form. We show that by adding spatial and temporal noise to the levels of an important regulator of external cAMP levels, the cAMP phosphodiesterase inhibitor, we can explain the natural progression of the system from randomly firing cells to circular waves whose symmetries break to form double- and single- or multi-armed spirals. When phosphodiesterase inhibitor is increased with time, mimicking experimental data, the wavelength of the spirals shortens, and a proportion of them evolve into pairs of connected spirals. We compare these results to recent experiments, finding that the temporal and spatial correspondence between experiment and model is very close.

Perhaps the most striking single feature of the *Dictyostelium discoideum* life cycle is the ability of the amoebae to self-organize and produce well-spaced territories that will later differentiate into highly structured fruiting bodies (1, 2). Self-organization begins when a few scattered cells spontaneously secrete a single pulse of cAMP (3–5). Cells in the surround respond by secreting more cAMP (2, 6) and begin to move toward the cAMP source (7, 8). cAMP diffuses to the next layer of cells, inducing a similar response, while the remaining cAMP is degraded by an external phosphodiesterase (PDE) (9) regulated by its inhibitor (PDI) (10–12); both proteins are secreted by the cells. The net result is a cAMP wave spreading outward from the excited cells.

Cell signaling produces characteristic bands of light and dark rings and spirals as territories begin to form (7, 13–15). It is known that the light bands correspond approximately to high cAMP concentrations (16). An example of the evolution of these patterns is shown in Fig. 1.

Although the evolution of spirals from preexisting spirals or broken wave segments has been modeled by Tyson and co-workers (18) and others (19), very little is known about how they emerge from biologically plausible initial conditions, why there are target patterns in some areas of a field of excitable cells and spirals in others, why some laboratory conditions appear to favor one over the other, and why for a particular strain and circumstance one pattern tends to dominate (20). These are important questions because they bear on early events governing the organization of the slime mold fruiting body. In addition, circular and spiral waves are generic to excitable systems, and thus an understanding of their origins in slime molds has wider applicability—for example, understanding spiral and planar waves in cardiac muscle (21, 22), the Belousov–Zhabotinskii reaction (23), Ca<sup>2+</sup> waves in *Medaka* eggs (24), and mitochondrial activity in *Xenopus* oocytes (25).

Here we show that PDI, a key protein of the intercellular signaling pathway, can have a major influence on the kinds of patterns observed. PDI is a 26-kDa glycoprotein that binds to PDE with a dissociation constant of  $\approx 10^{-10}$  M (12). We find that by regulating the inhibitor level, including stochastic variations in space or time, the emergence and evolution of circular and spiral patterns can be plausibly modeled. More generally, local increases in PDI levels serve as randomly distributed catalysts, initiating spontaneous excitations, while average global levels of PDI affect the excitability of the system as a whole.

## The Model

Our model is based on a kinetic scheme proposed by Martiel and Goldbeter (26) and further adapted by Tyson *et al.* (18) to include a spatial term. We use this model because it reproduces the essential properties of the signaling system, such as excitability, oscillation, and adaptation, even though the kinetic expressions of the Martiel and Goldbeter scheme do not correspond exactly to the complex biochemistry of the signaling system, still not completely understood (27, 28).

The observed properties of the cAMP signaling system and our choice of experimental parameters is described (18, 26). The simplified analytical version of the full model for amoebae on a surface, modified to account for changes in PDI levels, is

$$\frac{d\beta(x,y,t)}{dt} = s\Phi(\rho,\gamma) - \beta k_i - \beta k_t \quad [1]$$

Rate of change in intracellular [cAMP] = Production of cAMP - Intracellular hydrolysis - Secretion of cAMP

$$\frac{d\gamma(x,y,t)}{dt} = \frac{k_i}{h}\beta - k_e\gamma + D\nabla^2\gamma \quad [2]$$

Rate of change in extracellular [cAMP] = Secretion of cAMP - Extracellular hydrolysis + Diffusion of cAMP

$$\frac{d\rho(x,y,t)}{dt} = f_2(\gamma)(1 - \rho) - f_1(\gamma)\rho \quad [3]$$

Rate of change in fraction of active receptor = Dephosphorylation of receptor - Phosphorylation of receptor

$$k_e(x,y,t) = \frac{k_{e,\max}}{1 + \text{PDI}(x,y,t)} \quad [4]$$

Activity of phosphodiesterase = Effect of phosphodiesterase inhibitor

In Eq. 4,  $k_e$ , the activity of PDE, depends on  $k_{e,\max}$ , the uninhibited activity of PDE, and inversely on the concentration of PDI. The value  $k_e$  is critical, and in the model we regulate it by varying local PDI levels. We justify this by

Abbreviations: PDE, 3',5'-cAMP phosphodiesterase; PDI, inhibitor of PDE.

The publication costs of this article were defrayed in part by page charge payment. This article must therefore be hereby marked "advertisement" in accordance with 18 U.S.C. §1734 solely to indicate this fact.

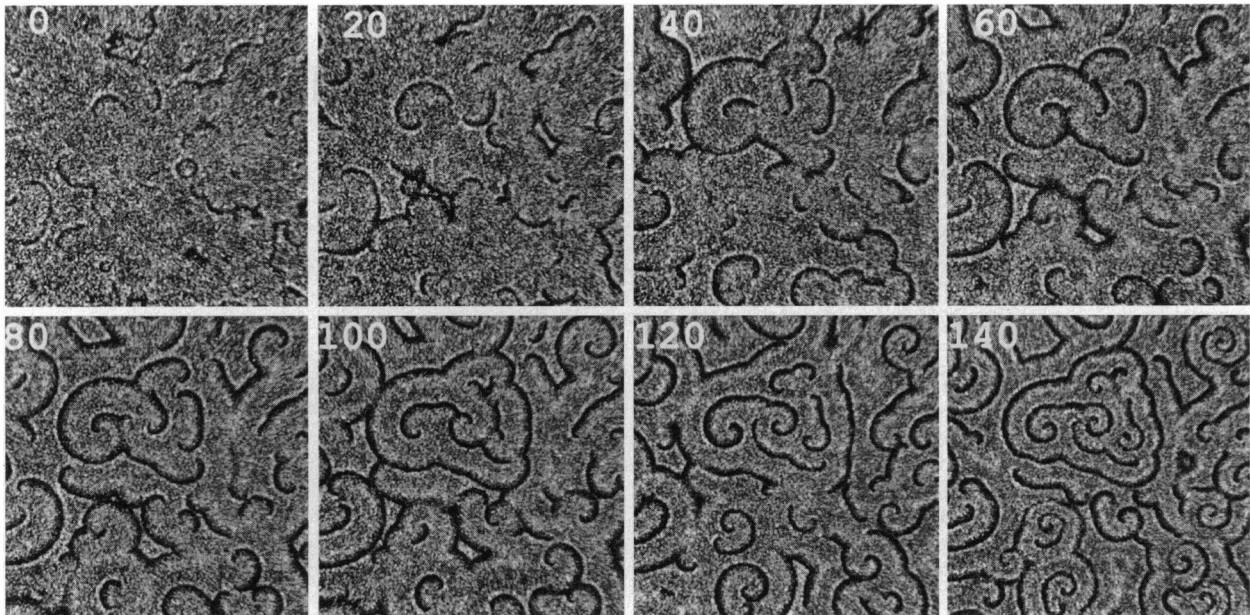


FIG. 1. Time lapse (min) data of *D. discoideum* amoebae aggregating on a thin layer of agar. Field is  $18 \times 18$  mm; dark-field optics. Cells plated at a density  $\rho = 2 \times 10^6$  cells per  $\text{cm}^2$  (K. Lee, E.C.C., and R. Goldstein, unpublished data). See ref. 17 for experimental details.

observing that shortly after the onset of starvation, cells begin to secrete PDI (12, 29). They are also caught at different times in their cell cycle as they begin to starve and thus exist in different biochemical states. We therefore assume the cells do not begin secreting PDI at the same time, and this gives rise to local heterogeneities in PDI levels. These initial processes and the resulting patterns formed occur very early during aggregation, before significant cell movements (7). Later, when cAMP waves are established, and the cells have experienced a number of successive pulses of cAMP, other processes are initiated, PDI secretion is halted, PDE levels rise, and the number of cAMP receptors increases (30). These events, along with cell movement, also affect pattern evolution, but much later.

The spontaneous release of cAMP pulses was modeled by assigning a probability  $p$  per time interval that an individual cell will pulse, and we show below that spontaneous increases in PDI levels can trigger this pulse. With time, as cAMP waves become established, neighboring cells become entrained and no longer secrete cAMP spontaneously. This was simulated by setting  $p = 0$  after 1000 time steps.

## Results

**Signaling in Well-Mixed Cell Suspensions.** Martiel and Goldbeter (26) modeled a stirred suspension of amoebae and found that the signaling system exhibited sustained cAMP oscillations under certain conditions of receptor density. We keep the number of receptors constant and explore the effect of changes in PDI levels. For well-stirred suspensions—i.e., no spatial terms in Eq. 1–4—our results are very similar to those obtained by these authors (Fig. 2). Here the level of PDI was spontaneously increased and then slowly reduced, to simulate the effect of PDI diffusion away from the source, which occurs in a field of cells. This pulse induces all of the amoebae to secrete cAMP (Fig. 2A). If the PDI levels remains high, the population secretes cAMP pulses periodically (Fig. 2B). It should be noted that the response of a stirred suspension of cells is equivalent to the response of a single cell in the same environment.

**Random Initial PDI Levels.** With these results in hand, we can now use the full model to explore patterning in a layer of excitable cells. For a field of cells, the initial PDI levels were

varied about a mean value in a random fashion (Fig. 3). For the first 1000 time steps, randomly distributed cAMP pulses were initiated. A pulse of cAMP, secreted by one or more cells, diffuses to adjacent cells, which respond in turn by secreting more. The cells first in this cascade then become refractory, while cells downstream respond by producing more cAMP. This process continues, and the net result is a circular wave of cAMP traveling away from the initiating cells.

Pulses initially give rise to circular waves (frame 2), which interact with new pulses. These interactions leave small semi-circular remnants (broken circles; arrows at frames 4 and 8), which evolve into double spirals (arrowheads, frames 8 and 16). Both regenerate and collide, often generating multiarmed spirals. In this simulation, two-armed spirals predominate (arrow in frame 64). In all of the examples shown in Fig. 3, waves spread from a pulse of cAMP, but the cell (or cells) that emit the pulse are not themselves oscillators. By and large they fire once and then subside. Waves persist and evolve because the end of a broken circle can persist in the absence of an oscillator (31).

How do circular waves break up to form spirals? When cAMP waves collide they annihilate, since cells on both sides of a wave are refractory to cAMP stimulation. Thus, collision between two waves cannot explain the origin of spirals. Rather, they form when a new pulse is emitted shortly after a wave has passed. When this happens, double spirals form (Fig. 4).

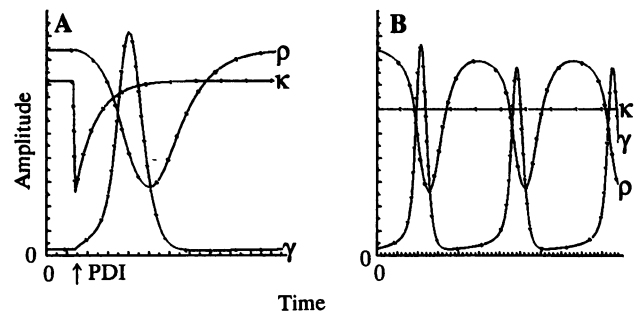


FIG. 2. Oscillations in suspensions of amoebae.  $\gamma$ , External [cAMP];  $\rho$ , fraction of receptor in active form;  $\kappa$ ,  $k_c$  activity. (A) We begin with  $k_c = 3.58$  and then set  $k_c = 1.25$ . It then returns exponentially to 3.58. (B)  $k_c = 3.0$  throughout the simulation.



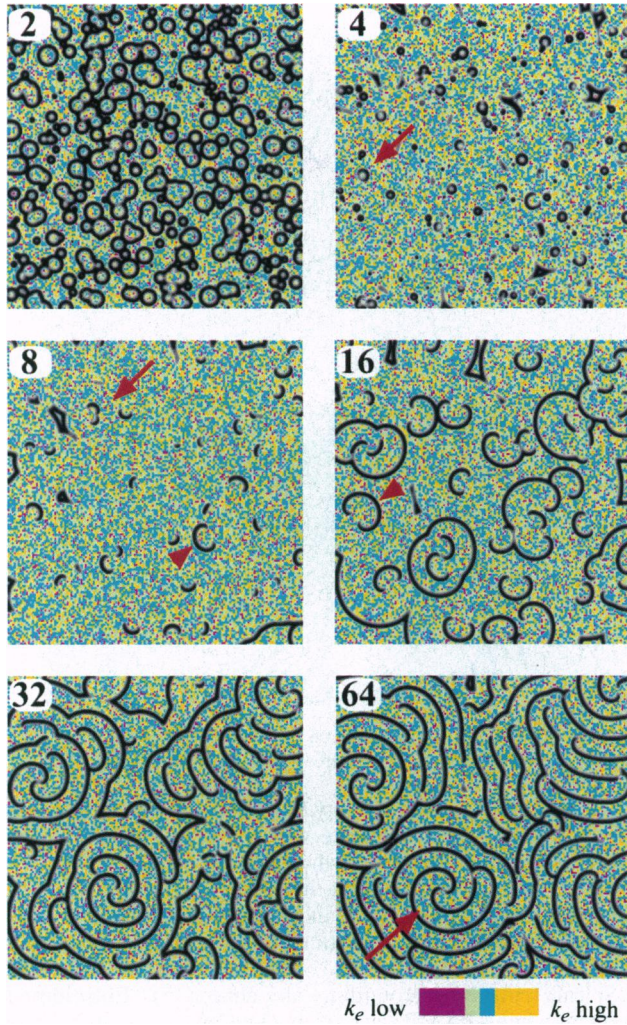


FIG. 3. Evolution of spirals from randomly firing amoebae. PDI varies spatially (stippled background, enlarged four times in the  $x, y$  plane for purposes of illustration) and does not change during the simulation. Numbers indicate frame number in the sequence (there are 200 computational steps between each frame number). Stippled background represents variations in activity of  $k_e$ . Values above and below  $1 \sigma$  are yellow and violet, respectively. Green and blue bars =  $1 \sigma$ . For the first 1000 time steps, the probability of a cAMP pulse was  $p = 2 \times 10^{-6}$  per grid point per time step, after which the pulses were stopped and waves were allowed to evolve. In frames 4–16, arrows point to broken circles and arrowheads point to double spirals. In frame 64, the arrow points to a two-armed spiral.  $k_e = 3.53 \pm 0.13$  ( $\pm 1 \sigma$ ). Grid was  $600 \times 600$ ;  $dx, dy = 0.1$  mm;  $dt = 0.04$  min.

The second pulse (frame 25) would normally give rise to a circular wave, but since the cells in the wake of the first wave are still in their refractory period, propagation in that direction is halted. Thus, a wave in the form of a half circle is created (Fig. 4, frame 35). The ends of the half circle begin to curl inward, and a double spiral begins to form (Fig. 4, frames 45 and 60). The arms of the double spiral continue to curl (Fig. 4, frame 75) and eventually collide and annihilate one another. The ends, however, survive (Fig. 4, frame 90) and again generate a new double spiral. The process repeats itself. The resulting pattern is a double spiral in the center of concentric elliptical waves of cAMP. Notice that the double spiral regenerates. There is no need for a pulse or pacemaker. This regenerating quality is true in general for spirals in excitable media.

**Uniform Increase in PDI Concentrations.** It is known that early during aggregation, levels of PDI increase (12, 29). We explored

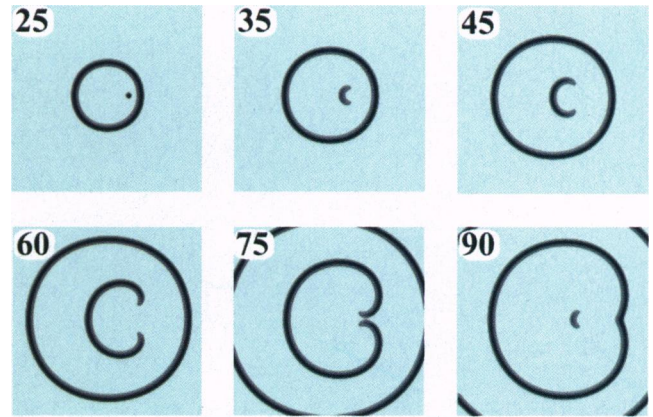


FIG. 4. Formation of double spirals by interaction of a new pulse with a recently passed wave. Numbers indicate frame (there are 25 computational steps between each frame number). A cAMP pulse is initiated at frame 25 and gives rise to a double spiral (frame 45). Double spiral regenerates and forms the beginning of a new double spiral (frame 90).  $k_e = 3.58$  uniformly.

the effect of a uniform increase in PDI levels by raising it incrementally and uniformly at each time step (Fig. 5).

As before, there are random cAMP pulses for the first 1000 time steps, which quickly become centers for circular waves (frame 2). With time, double spirals form and persist. Their ends rotate in opposite senses, and the separation between adjacent arms (the wavelength) decreases (frames 22–72). By comparison of these results with Fig. 3, it is apparent that patterns are initiated in a similar manner. However, fewer double spirals form, partly because the initial excitability is lower and partly because the probability,  $p$ , of a spontaneous cAMP pulse is lower. At intermediate stages (frames 32–62), double spirals tighten and the wavelength decreases, behavior that is not seen in Fig. 3. Finally, the longer term outcome is often pairs of connected spirals rotating in opposite directions (arrow in frame 72). There is significant change in both the wavelength and rotational period as PDI levels increase.

## Discussion

We suggest that the early patterns seen in fields of starving *D. discoideum* amoebae can be explained rather simply in terms of spatial and temporal heterogeneity of PDI concentrations. We adapted the models first proposed by Martiel and Goldbeter (26) and extended by Tyson *et al.* (18) to contain the effect of variations in one of the parameters known to be involved in morphogenesis in *D. discoideum*. By observing that at some time point after onset of starvation a cell will begin to secrete PDI, we can explain the seemingly random spontaneous cAMP pulses observed in a field of aggregating amoebae. From these assumptions, we can show how circular waves of cAMP give rise to spiral waves and how spiral waves evolve in their substructure. An increase in local PDI level can lead to emission of a cAMP pulse; local random PDI increases in space and time result in the appearance of circular waves of cAMP originating at random times and positions; interactions between these waves and new pulses often lead to the formation of double spirals, which due to asymmetries in the surroundings caused by variations in PDI develop into single- and multiarmed spirals. It should be noted that the location of the spiral center differs from the location of the center of the circular waves. The cells that signal first do not necessarily form the core of the spiral.

It is worth pointing out that the system we study is an excitable system, most of whose properties are generic. In chemical systems, such as the Belousov–Zhabotinskii reaction, patterns originate from inhomogeneities in the surroundings,



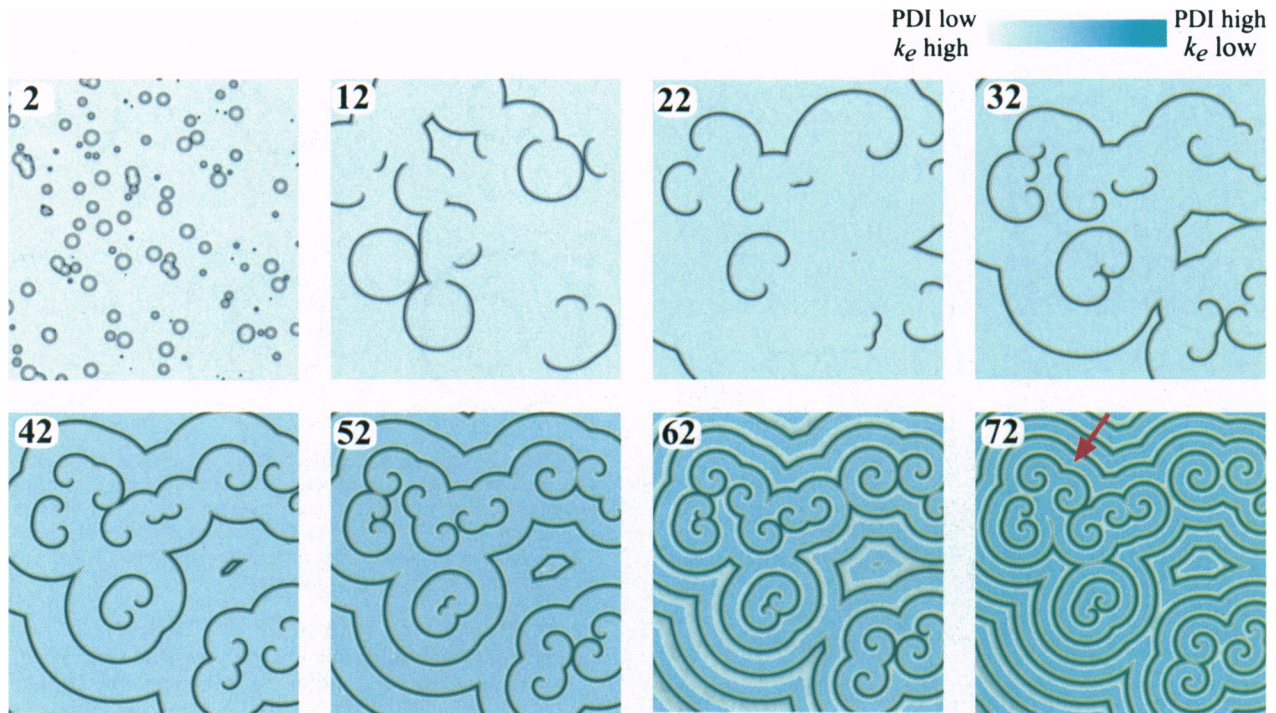


FIG. 5. Continuously increasing levels of PDI influence the outcome.  $k_e$  was decreased each time step from  $k_e = 3.73 \pm 0.13$  to  $k_e = 2.88 \pm 0.13$ . Note that  $k_e \approx 1/\text{PDI}$ . Probability of a firing event at a grid point was  $0.5 \times 10^{-6}$ . Other conditions are as described in Fig. 3.

which function as seeds from which waves will originate (32). For *D. discoideum*, in contrast, the inhomogeneities of the system arise from heterogeneity of the cells themselves. Physiological properties evolve during development, and therefore the inhomogeneities and the excitability of the system also change. This is a characteristic of biological systems—the system evolves in time until the conditions necessary for pattern formation have been reached. Thus, in biological systems, time-dependent internal variables often play a crucial role in pattern formation. These variables may depend on time only, or they can also be affected by the evolving patterns themselves—e.g., cAMP waves induce production of PDE and receptors while inhibiting PDI production.

When we included the effect of gradually increasing the overall PDI levels in our simulation, we observed double spirals whose wavelengths decreased, and rotational speeds increased with time, often resulting in a pair of connected spirals (Fig. 5). This is in excellent agreement with the experimental results shown in Fig. 1, where the cells were harvested, washed, and deposited in a uniform layer on an agar surface (17). It is also clearly illustrated in the experiments of Tomchik and Devreotes (16).

A decrease in wavelength and period during aggregation has been demonstrated experimentally (13, 15). These authors also showed a decrease in the cAMP wave speed, which we do not observe in our simulations. However, the data from Fig. 1 do not indicate a significant change in wave speed for the first 150 min. Both wavelength and period do decline later (K. Lee, personal communication). Early on, the global increase in PDI levels shortens the period of the spirals. At the same time, high PDI levels make the system more excitable, which works against the usual decrease in wave speed following a decrease in period. Later, PDI secretion stops (30), and the continuing shortening of the wave length may be caused by other factors, such as increased density around the spiral center, which locally increases the excitability but does not affect the rest of the system. This reduces the wave speed, according to general dispersion relations of excitable media (18).

When amoebae are grown on a carpet of bacteria, there is considerable large scale heterogeneity in starvation condi-

tions, cell age, and cell density, and single armed spirals are common (14). This, we believe, is the expected result, since if a double spiral is formed where each arm experiences a different average level of PDI, it will turn into a single armed spiral (data not shown). This happens because the arm experiencing higher PDI levels rotates faster and eventually dominates the other arm.

Spirals entrain surrounding amoebae (17). Entrainment happens when a cAMP wave from a nearby center periodically impinges upon neighboring amoebae. Entrainment prevents further pulsing, and as a consequence new centers do not form. This effect can be seen in Fig. 5, where the average value of  $k_e$  is low enough to induce formation of pacemakers. However, existing spirals prevent spontaneous oscillations. New centers must therefore form before all the amoebae on the plate are entrained. In this work, spontaneous cAMP pulses were initiated by directly elevating external cAMP levels, and later entrainment was assumed by setting  $p = 0$ . Similar results are obtained if pulsing is driven by PDI levels directly (unpublished observations).

For any given region there exists a probability of a cAMP pulse, although which cells serve as the source is unpredictable. Clearly, the probability is affected by the density and the developmental stage of the cells. We are not aware of experimental data that would allow us to determine the value of  $p$ . However, we did explore the effect of changes in  $p$  (data not shown). Increasing  $p$  raises the frequency of random pulses and consequently leads to more wave-pulse interactions, which results in the formation of an increasing number of double spirals. Lowering the value of  $p$  results in fewer cAMP pulses and therefore fewer double spirals. In one limit, when the value of  $p$  becomes too low, double spirals do not form (data not shown). These results are also in accord with recent observations (17).

When cell density is low, the initial value of  $p$  is not high enough to allow the formation of double spirals. Thus, we predict that local levels of PDI will eventually increase sufficiently and remain high locally, turning some cells into pacemakers and resulting in the formation of mostly target patterns. If we add PDI, we should trigger the signaling system

prematurely and thus initiate pattern formation in a younger system. Increasing PDI levels locally should also result in formation of target patterns. Mutants in both PDE and PDI provide a means of manipulating the signaling system (33, 34). For PDI knockouts, we predict that formation of the wave pattern will be delayed, relative to wild type. In PDI overexpressors or PDE knockouts, the cAMP levels will rise and saturate the receptors so that no cAMP waves can form. In mutants overexpressing PDE, cAMP waves cannot propagate and therefore should not be seen.

We have chosen PDI levels as an external variable, both to trigger cAMP waves and to change the geometry of waves and spirals with time. Is this an arbitrary choice? First, as noted above, it seems to be biologically realistic. PDI is synthesized and secreted into the medium early and before PDE secretion. Second, secretion of PDI not only affects the excitability of the secreting cell itself, but by diffusion affects neighbors as well, giving rise to a cAMP pulse from a group of cells. This cannot be achieved by PDE secretion, for example, because PDE secretion works the wrong way—at high PDE levels, the system becomes less excitable, not more. Other factors could also increase excitability and give rise to cAMP pulses, such as increased number of cAMP receptors or increased cell density. However, receptor number increases as a consequence of pulsing and increase in cell density does not occur until after cAMP patterns have formed.

In sum, this is a highly evolved system, and in our view PDI regulation achieves several goals: (i) it can initiate cAMP pulses; (ii) by diffusing locally it can enhance the probability that a signaling center will form; (iii) it can increase globally the excitability of the system; and (iv) once territories have become established, it is no longer synthesized. At this point, other factors begin to influence the system.

We thank Ray Goldstein and Kyoung Lee for helpful discussion and unpublished results; Giselle Thibaudeau for help with the manuscript; and Petra Fey, Keqin Gregg, George Hurrt, and Simon Levin for other suggestions. This work was supported by grants from the National Science Foundation (IBN 93-04849) and in part by the Materials Research Science and Engineering Center Program of the National Science Foundation under Award DMR 94-00362.

1. Shaffer, B. M. (1962) *Adv. Morphog.* **2**, 109–182.
2. Bonner, J. T. (1967) *The Cellular Slime Molds* (Princeton Univ. Press, Princeton), 2nd Ed.
3. Konijn, T. M., van de Meene, J. G. C., Bonner, J. T. & Barkley, D. S. (1967) *Proc. Natl. Acad. Sci. USA* **58**, 1152–1154.

4. Gerisch, G., Malchow, D. & Hess, B. (1974) in *Biochemistry of Sensory Functions*, ed. Jaenicke, L. (Springer, New York), pp. 279–298.
5. Devreotes, P. N. & Steck, T. L. (1979) *J. Cell Biol.* **80**, 300–309.
6. Shaffer, B. M. (1975) *Nature (London)* **255**, 549–552.
7. Alcantara, F. & Monk, M. (1974) *J. Gen. Microbiol.* **85**, 321–334.
8. Devreotes, P. N. (1982) in *The Development of Dictyostelium discoideum*, ed. Loomis, W. F. (Academic, New York), pp. 117–168.
9. Chang, Y. Y. (1968) *Science* **161**, 57–59.
10. Riedel, V., Malchow, D., Gerisch, G. & Naegelé, B. (1972) *Biochem. Biophys. Res. Commun.* **46**, 279–287.
11. Kessin, R. H., Orlow, S. J., Shapiro, R. I. & Franke, J. (1979) *Proc. Natl. Acad. Sci. USA* **76**, 5450–5454.
12. Franke, J. & Kessin, R. H. (1981) *J. Biol. Chem.* **256**, 7628–7637.
13. Gross, J. D., Peacey, M. J. & Trevan, D. J. (1976) *J. Cell Sci.* **22**, 645–656.
14. Newell, P. C. (1983) in *Attraction and Adhesion in the Slime Mold Dictyostelium*, ed. Smith, J. (Dekker, New York), pp. 43–71.
15. Siegert, F. & Weijer, C. (1989) *J. Cell Sci.* **93**, 325–335.
16. Tomchik, K. J. & Devreotes, P. N. (1981) *Science* **212**, 443–446.
17. Lee, K., Cox, E. C. & Goldstein, R. (1995) *Phys. Rev. Lett.*, **76**.
18. Tyson, J., Alexander, K., Manoranjan, V. & Murray, J. (1989) *Physica D (Amsterdam)* **34**, 193–207.
19. Hofer, T., Sherratt, J. A. & Maini, P. K. (1995) *Physica D (Amsterdam)* **85**, 425–444.
20. Durston, A. J. (1973) *J. Theor. Biol.* **42**, 483–504.
21. Jalife, J. & Antzelevitch, C. (1979) *Science* **206**, 695–697.
22. Davidenko, J. M., Pertsov, A. V., Salomonsz, R., Baxter, W. & Jalife, J. (1992) *Nature (London)* **355**, 349–351.
23. Zaikin, A. N. & Zhabotinskii, A. M. (1970) *Nature (London)* **225**, 535–537.
24. Jaffe, L. F. (1995) *Ciba Found. Symp.* **188**, 4–17.
25. Jouaville, S. L., Ichas, F., Holmuhamedov, E. L., Camacho, P. & Lechleiter, J. (1995) *Nature (London)* **377**, 438–441.
26. Martiel, J. L. & Goldbeter, A. (1987) *Biophys. J.* **52**, 807–828.
27. Caterina, M. J., Devreotes, P. N., Borleis, J. & Hereld, D. (1995) *J. Biol. Chem.* **270**, 8667–8672.
28. Lilly, P. J. & Devreotes, P. N. (1995) *J. Cell Biol.* **129**, 1659–1665.
29. Gerisch, G., Malchow, D., Riedel, V., Müller, E. & Every, M. (1972) *Nature (London) New Biol.* **235**, 90–92.
30. Yeh, R. P., Chan, F. K. & Coukell, M. B. (1978) *Dev. Biol.* **66**, 361–374.
31. Markus, M., Krafczyk, M. & Hess, B. (1991) in *Nonlinear Wave Processes in Excitable Media*, eds. Holden, A. V., Markus, M. & Othmer, H. G. (Plenum, New York), Vol. 244, pp. 161–182.
32. Maselko, J. & Showalter, K. (1991) *Physica D (Amsterdam)* **49**, 21–32.
33. Faure, M., Podgorski, G. J., Franke, J. & Kessin, R. H. (1988) *Proc. Natl. Acad. Sci. USA* **85**, 8076–8080.
34. Wu, L., Franke, J., Blanton, R. L., Podgorski, G. J. & Kessin, R. H. (1995) *Dev. Biol.* **167**, 1–8.